Josephson interferometer in a ring topology as a proof of the symmetry of Sr_2RuO_4

Yasuhiro Asano*
Department of Applied Physics, Hokkaido University, Sapporo 060-8628, Japan

Yukio Tanaka
Department of Applied Physics, Nagoya University, Nagoya 464-8603, Japan

Manfred Sigrist
Theoretische Physik, ETH Honggerberg, 8093 Zurich, Switzerland

Satoshi Kashiwaya
National Institute of Advanced Industrial Science and Technology, Tsukuba 305-8568, Japan
(Received 2 February 2005; published 1 June 2005)

The Josephson effect is theoretically studied in two types of SQUIDs consisting of *s* wave superconductor and Sr_2RuO_4. Results show various response of the critical Josephson current to applied magnetic fields depending on the type of SQUID and on the pairing symmetries. In the case of a p_x+ip_y wave symmetry, the critical current in a corner SQUID becomes an asymmetric function of magnetic fields near the critical temperatures. Our results well explain a recent experimental finding [Nelson *et al.*, Science **306**, 1151 (2004)]. We also discuss effects of chiral domains on the critical current.

DOI: 10.1103/PhysRevB.71.214501 PACS number(s): 74.50.+r, 74.25.Fy, 74.70.Tx

I. INTRODUCTION

One of the important developments for unconventional superconductivity after the the discovery of high-T_c superconductivity,[1] has been the series of so-called phase sensitive experiments which test for the symmetry of the Cooper pair wave function. These are the SQUID-type of interference experiments,[2–5] the observation of spontaneous half-flux quantization in frustrated loops[6] and the measurement of zero-bias peaks in quasiparticle tunneling spectra indicating subgap quasiparticle states at the sample surface.[7–11] This set of experiments, technically rather diverse, is based on the same concept, the unconventional phase structure of the superconducting condensate, and have uniquely proven that the Cooper pairs have the spin-singlet $d_{x^2-y^2}$ wave symmetry. A further unconventional superconductor whose pairing symmetry has been established with high confidence is Sr_2RuO_4.[12] This is a spin triplet *p*-wave superconductor[13–15] with a gap function of the form $\boldsymbol{d}(\boldsymbol{k}) \propto \hat{\boldsymbol{z}}(p_x \pm ip_y)$,[16,17] a so-called chiral *p*-wave state with whose Cooper pairs possess an angular momentum component along the *z* axis. Tunneling experiments have shown the presence of subgap surface states.[18,19] Moreover, the anomalous temperature dependence of the critical current in $Pb/Sr_2RuO_4/Pb$ Josephson junction arrangement[20] has been interpreted in terms of an interference effect.[21–23] A direct experiment of the type of a SQUID-interference or frustrated loop is difficult here for many technical reasons and has not been performed until very recently.[24]

In this paper we would like to analyze some issues which have to be taken into account in the interpretation of the SQUID-type experiments for Sr_2RuO_4. The basic principle had been designed long ago by Geshkenbein and co-workers.[25] One of the problems lies in the Josephson junctions between a conventional spin-singlet *s*-wave superconductor and a spin-triplet *p*-wave superconductor. The mismatch of the angular moment (parity) and of spin quantum number on the two sides of a Josephson junction seems at first sight inhibit the lowest order Josephson effect so that only a coupling in second order would be allowed. This would indeed be fatal for phase sensitive tests based on the Josephson effect. It has, however, been shown that the presence of spin-orbit coupling saves the situation since only the total angular momentum has to be conserved. Thus under well-defined conditions, the lowest order between an *s*- and a *p*-wave superconductor is possible.[26–30] The conditions leave a certain arbitrariness concerning the sign of the Josephson coupling which can be important for interference effects. This can be illustrated, if we consider the definition of the lowest order matrix element which can be derived from a simple microscopic tunneling model:

$$\langle \psi_s(\boldsymbol{k})(\boldsymbol{k}\times\boldsymbol{n})\cdot\boldsymbol{d}(\boldsymbol{k})\rangle_{\mathrm{FS}}, \tag{1}$$

where the average runs over the Fermi surface and $\boldsymbol{n}$ is the interface normal vector. The arbitrariness appears in the orientation of the normal vector, into or out of the *p*-wave superconductor. This has been recently demonstrated by Asano and co-workers[30] for a model where the spin-orbit coupling of the interface potential was taken into account for this matrix element whose sign then depends on the shape of the interface potential. Thus details of the spin-orbit coupling and the interface potential, e.g., the way the parity is broken at the interface, matter for the Josephson phase relation. The arrangement suggested by Geshkenbein *et al.* relies on the assumption that all interfaces treat parity the same way.[25] We will follow this assumption here too.

We discuss now two basic forms of SQUID-interference devices built from an *s*- and a *p*-wave superconductor. The first type in Fig. 1(a) is the symmetric SQUID as proposed

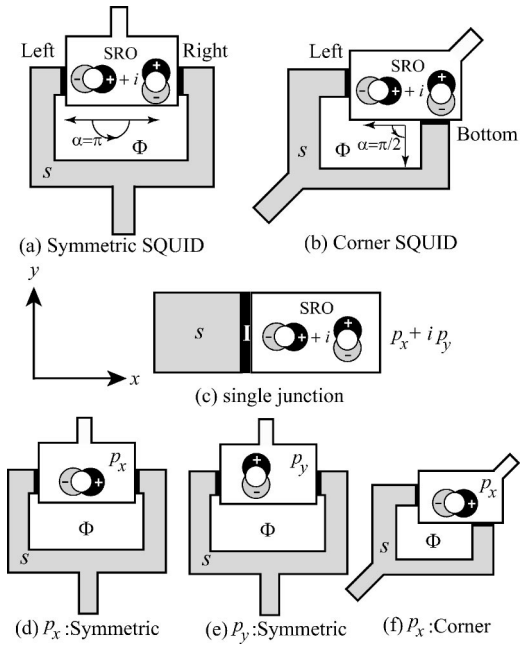

FIG. 1. Schematic pictures of two types of Josephson junction are shown in (a) and (b). The singly connected Josephson junction is given in (c). In (d)–(f), the SQUID of p_x and p_y symmetries are shown. The Josephson effect in the corner SQUID of p_y symmetry is identical to that of the p_x symmetry.

by Geshkenbein and co-workers[25] and the second in Fig. 1(b) is the corner-SQUID analogous to the one used for high-T_c superconductors. The p_x+ip_y phase of Sr_2RuO_4 introduces an additional problem. This phase is twofold degenerate, i.e., p_x+ip_y and p_x-ip_y are equivalent and would in general form domains in a sample, depending on the cooling history. We will discuss in the following also the implications domains on the interference experiment. Similar problems appear for other chiral superconducting phase as we will discuss below.

This paper is organized as follows. In Sec. II, the Josephson effect in two types of SQUID is discussed for p_x+ip_y, p_x and p_y pairing symmetries. Effects of the chiral domain are studied in Sec. III. In Sec. IV, we discuss the critical current in the chiral *d* and the chiral *f* wave symmetries. The discussion and the conclusion are given in Secs. V and XI, respectively.

II. JOSEPHSON CURRENT

Before discussing the SQUID-experiment, the basics of the Josephson current-phase relation between *s* wave superconductor and Sr_2RuO_4 (SRO) in Fig. 1(c) has to be addressed. We describe the gap function of Sr_2RuO_4 by[16,31]

$$\hat{\Delta}_{\boldsymbol{p}} = i(\eta_x \overline{p_x} + \eta_y \overline{p_y})\hat{\boldsymbol{z}} \cdot \hat{\boldsymbol{\sigma}}\hat{\sigma}_2, \tag{2}$$

$$= i\Delta(\overline{p_x} \pm i\overline{p_y})\hat{\boldsymbol{z}} \cdot \hat{\boldsymbol{\sigma}}\hat{\sigma}_2 \tag{3}$$

$$= i\Delta e^{i\theta}\hat{\boldsymbol{z}} \cdot \hat{\boldsymbol{\sigma}}\hat{\sigma}_2, \tag{4}$$

where $\hat{\sigma}_j$ with $j=1$, 2 and 3 are the Pauli matrices, η_x and η_y are the two complex order parameters and $\hat{\boldsymbol{z}}$ is taken as a unit vector parallel to the *z* axis.[17] Moreover, $\overline{p_x}=p_x/p_F=\cos\theta(\overline{p_y}=p_y/p_F=\sin\theta)$ is the normalized momentum component on the Fermi surface in the $x(y)$ direction with p_F being the Fermi momentum of the *p*-wave superconductor. Assuming a cylindrical symmetric Fermi surface, we can represent this gap function also simply to the angle θ on the Fermi surface, reflecting best its internal phase structure. The gap function of the *s*-wave superconductor is given by $\hat{\Delta}_{\boldsymbol{k}}=i\Delta\hat{\sigma}_2$. Without any loss of generality, we may take the gap magnitudes identical in both superconductors, Δ. On the basis of the current-phase relation,[27–29] the Josephson current for the lowest two orders derived from a microscopic calculation close to T_c[30] can be written as

$$\overline{J}_{p_x \pm ip_y} = J_1\cos(\varphi + \theta_n) - J_2\sin(2(\varphi + \theta_n)), \tag{5}$$

$$J_1 = T_B\alpha_S\left(\frac{\Delta}{2T}\right)\frac{\Delta}{\Delta_0}, \tag{6}$$

$$J_2 = T_B^2\left(\frac{\Delta}{2T}\right)^3\frac{\Delta}{\Delta_0}, \tag{7}$$

where θ_n is the angle of the junction normal vector in the plane relative to the *x* axis, T_B denotes the transmission probability of a Cooper pair and α_S is a measure for the strength of the spin orbit coupling. Note that it can have either sign depending on the junction. The Josephson current $\overline{J}$ is measured in units of $e\Delta_0 N_c/\hbar$, where Δ_0 is the amplitude of the gap function at $T=0$ and N_c is the number of propagating channels on the Fermi surface. Constant coefficients of the order of unity have been omitted in Eq. (5). From Eq. (1) it is clear that the coupling between *s*-wave and p_x+ip_y-wave superconductor for a junction in *x* direction ($\theta_n=0$) goes via the p_y component. We assume a gauge where the overall phase of the *p*-wave order parameter is shifted by $\pm\pi/2$ for the p_y component. Thus, in lowest order the current-phase relation is proportional to $\cos\varphi$ rather than $\sin\varphi$, in Eq. (5).

In the first step, we consider the interference pattern of the two basic SQUID's in Figs. 1(a) and 1(b). We assume that all junctions are of the same in the sense, that the normal vector $\boldsymbol{n}$ in Eq. (1) is pointing a definite direction, say towards the *s*-wave superconductor. In the symmetric SQUID, the Josephson current of the left and right junction are given by

$$J_L(\varphi) = J_1\cos\varphi - J_2\sin 2\varphi, \tag{8}$$

$$J_R(\varphi) = -J_1\cos\varphi - J_2\sin 2\varphi. \tag{9}$$

The relative sign change between the first-order terms on both sides is due to the the corresponding θ_n which differ by π. The Josephson current in the symmetric SQUID is then expressed by[32]

$$J_S(\varphi,\Phi) = J_L(\varphi + \phi_B) + J_R(\varphi - \phi_B), \tag{10}$$

$$= -2J_1\sin\varphi\sin\phi_B - 2J_2\sin 2\varphi\cos 2\phi_B, \tag{11}$$

where $\phi_B=\pi\Phi/\Phi_0$ and $\Phi_0=2\pi\hbar c/e$. In the corner SQUID,

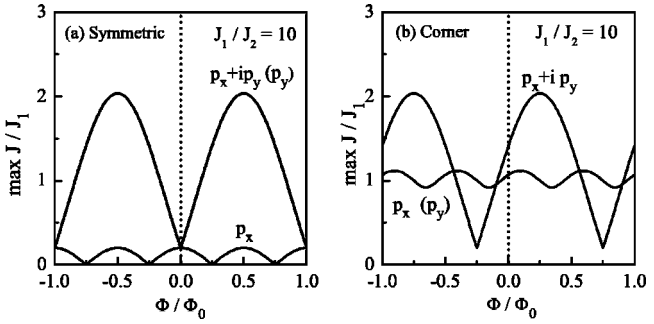

FIG. 2. The Josephson critical current is plotted as a function of Φ in the symmetric SQUID in (a) with $J_1/J_2=10$. The calculated results for the corner SQUID are shown in (b).

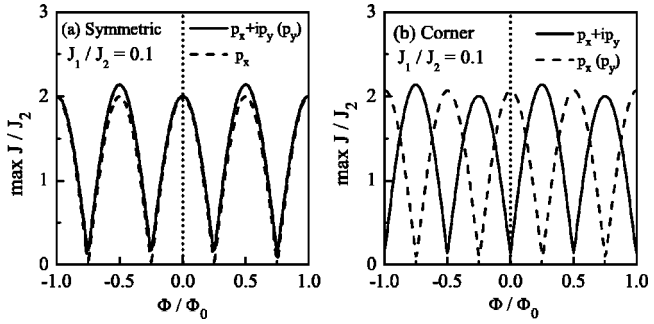

FIG. 3. The Josephson critical current is plotted as a function of Φ for $J_1/J_2=0.1$.

the Josephson current in the bottom junctions is given by

$$J_B(\varphi) = -J_1 \sin\varphi + J_2 \sin 2\varphi, \tag{12}$$

where the current-phase relation is derived from Eq. (5) with $\theta_n=\pi/2$. The Josephson current in the corner SQUID is expressed in the same way,

$$J_C(\varphi,\Phi) = J_1\cos(\varphi+\phi_B) - J_1\sin(\varphi-\phi_B) - 2J_2\cos 2\varphi \sin 2\phi_B. \tag{13}$$

Note that for the corner SQUID it matters which state is realized. For Eq. (12) we assumed that the state p_x+ip_y, while for p_x-ip_y would yield a sign change of the first term.

In Fig. 2, the critical Josephson current in the symmetric SQUID and that in the corner SQUID are shown as a function of Φ. A parameter $J_1/J_2=10$ is realized in high temperatures near T_c. Since $J_1 \gg J_2$, we find

$$\max|J_S(\Phi)| \simeq 2J_1 \left|\sin\left(\pi\frac{\Phi}{\Phi_0}\right)\right|, \tag{14}$$

$$\max|J_C(\Phi)| \simeq 2J_1 \left|\sin\left(\pi\frac{\Phi}{\Phi_0} \pm \frac{\pi}{4}\right)\right|. \tag{15}$$

The odd parity symmetry immediately results in a minimum of the critical current at $\Phi=0$ in the symmetric SQUID,[25] which is connected with the opposite sign of Josephson coupling on the two junctions according to Eq. (9). Note that this pattern is not dependent on which of the two degenerate *p*-wave state is realized. Actually for the symmetric SQUID any *p*-wave pairing state gives the same qualitative behavior and does not depend on the detailed symmetry, such as broken time reversal symmetry, as long as the first-order Josephson coupling induced by spin-orbit effects is dominant. This is different for the corner SQUID which leads to a distinction between different *p*-wave states.

The change to the corner SQUID configuration yields a phase shift by $\pm\pi/2$ for $p_x\pm ip_y$. As a consequence, the $\cos\varphi$ current-phase relation can be exchanged by $\sin\varphi$ for the bottom junction. For comparison, the results for the p_x- and p_y-wave states are depicted in Fig. 2 with the corresponding device illustrations in Figs. 1(d)–1(f). The Josephson current-phase relation in the single junctions can for fixed gauge be given by[30,33]

$$J_{p_x}(\varphi) = -J_2 \sin 2\varphi, \tag{16}$$

$$J_{p_y}(\varphi) = J_1\sin\varphi - J_2\sin 2\varphi. \tag{17}$$

For the p_x component (***n*** parallel to *x*), there is no contribution due to spin-orbit coupling, in contrast to the p_y component which has such a term proportional to $\sin\varphi$. in the p_y symmetry.

In the symmetric SQUID of the p_x type, the critical current has the period of $\Phi_0/2$ as shown in Fig. 2(a) because there is only the second-order contribution in the Josephson coupling. On the other hand, the p_y type behaves identical to the p_x+ip_y type. For the corner SQUID configuration the p_x symmetry (and equivalently for the p_y symmetry) has again a $\Phi_0/2$-periodic interference pattern of the critical current.

If we assume that $J_1 \ll J_2$ due to weak spin-orbit coupling, the features of the interference pattern are significantly modified. In Fig. 3, the critical Josephson current is plotted as a function of Φ for $J_1=0.1J_2$. For $J_1 \ll J_2$, we actually find

$$\max|J_S(\Phi)| \simeq 2J_2 \left|\cos\left(2\pi\frac{\Phi}{\Phi_0}\right)\right|, \tag{18}$$

$$\max|J_C(\Phi)| \simeq 2J_2 \left|\sin\left(2\pi\frac{\Phi}{\Phi_0}\right)\right|, \tag{19}$$

for the p_x+ip_y symmetry. The period of J_c is given by $\Phi_0/2$ because the Josephson current proportional to $\sin 2\varphi$ is dominant. The critical current in the symmetric SQUID takes its maxima at $\Phi=0$ because $\sin 2\varphi$ remains unchanged under the π phase shift. On the other hand in the corner SQUID, the critical current takes its minima at $\Phi=0$. This is due to the sign change of $\sin 2\varphi$ under the $\pi/2$ phase shift in the p_x+ip_y symmetry. The critical current in the p_x and p_y symmetries can be described by Eq. (18) irrespective of types of SQUID as shown in the Fig. 3. Thus the minima at $\Phi=0$ in the corner SQUID directly suggests the p_x+ip_y symmetry in SRO when the period of the oscillations is $\Phi_0/2$.

In Fig. 4, the critical current for the p_x+ip_y symmetry is shown for several choices of J_1/J_2. In the vertical axis, successive plots have been offset. The critical current is always symmetric with respect to Φ in the symmetric SQUID. The current maxima at Φ_0 for $J_1/J_2=0.1$ is changed to the

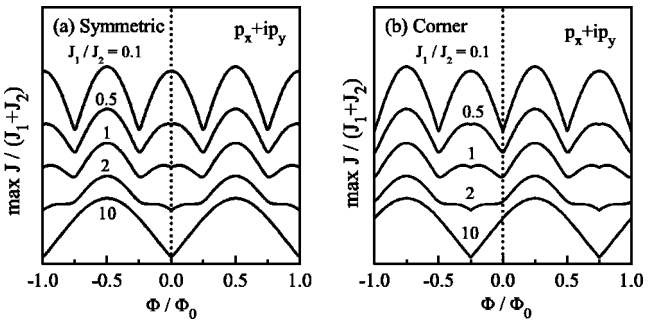

FIG. 4. The Josephson critical current is plotted as a function of Φ for p_x+ip_y.

minima as increase of J_1/J_2. In the corner SQUID, the asymmetry in the critical current gradually disappears with decreasing of J_1/J_2.

III. CHIRAL DOMAINS

We have assumed so far that SRO is a single domain of the p_x+ip_y symmetry. Real materials, however, may have multidomain structures of the p_x+ip_y and the p_x-ip_y symmetries. Here we discuss effects of chiral domains on the Josephson current. We consider a simple model of such chiral domains as shown in Fig. 5, where $\uparrow$ and $\downarrow$ indicate domains of the different chiral states. The size of domains should be much larger than the thickness of domain walls which is typically given by the coherence length of superconductors. The structure of domain walls has been investigated based on Ginzburg-Landau theories.[34] For a domain wall with normal vector $\boldsymbol{n}$, the p-wave component parallel to $\boldsymbol{n}$, $p_\parallel$, keeps its phase, while the component perpendicular, $p_\perp$, changes the phase by π. This has important implication

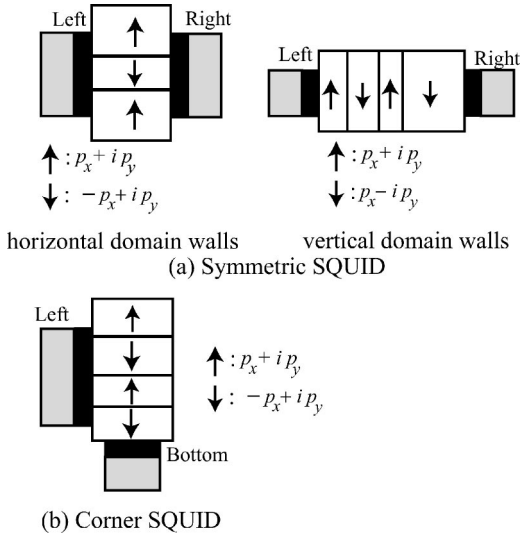

FIG. 5. A simple model of chiral domains is illustrated in the symmetric SQUID (a) and the corner SQUID (b). Across the domain wall with a normal vector $\boldsymbol{n}$, the p-wave component parallel to $\boldsymbol{n}$ keeps its phase, while the component perpendicular to $\boldsymbol{n}$ changes the phase by π.

to the analysis of the above SQUID configurations which we will discuss here for a few simple situations as shown in Fig. 5, under the assumption $J_1 \gg J_2$.

The presence of *horizontal* domain walls in Fig. 5, i.e., $\boldsymbol{n} \| y$, implies that the two chiral domains have either p_x+ip_y or $-p_x+ip_y$ form. According to our previous discussion, no qualitative change of the interference pattern is expected. Thus the critical current in Fig. 2(a) remains unchanged even in the presence of the horizontal domain walls in the symmetric SQUID. On the other hand, the vertical domain walls give rise to domains with p_x+ip_y and p_x-ip_y form. In this case the number for domain walls between the two junctions matters since each domain wall switches the phase of p_y, entering the first-order term of the Josephson coupling, by π. Thus the interference pattern would look different for an odd or even number of domain walls:

$$\max|J_S(\Phi)| \simeq \begin{cases} 2J_1\left|\sin\left(\pi\frac{\Phi}{\Phi_0}\right)\right| & N_{\mathrm{DW}} \text{ even}, \\ 2J_1\left|\cos\left(\pi\frac{\Phi}{\Phi_0}\right)\right| & N_{\mathrm{DW}} \text{ odd}, \end{cases} \tag{20}$$

where N_{DW} is the number of the vertical domain walls. If the number of walls is an even integer, the critical current takes its minimum at $\Phi=0$ as shown in Fig. 6(a). However, the critical current has its maximum at $\Phi=0$ when the number of domain walls is an odd integer. Thus the existence of the vertical domain walls can change drastically the characteristic feature of the critical current in the symmetric SQUID.

In the corner SQUID, the current-phase relation in the two junctions as shown in Fig. 5(b) are given by

$$J_L(\varphi) = J_1\cos\varphi - J_2\sin 2\varphi, \tag{21}$$

$$J_B(\varphi) = \pm J_1\sin\varphi + J_2\sin 2\varphi, \tag{22}$$

where the sign of the first-order term of the bottom junction is determined by the chirality of the last domain at the bottom. The number of domain walls is irrelevant here. Still the asymmetry of the interference pattern indicates the broken time reversal symmetry in any case as shown in Fig. 6(b).

IV. OTHER CHIRAL SUPERCONDUCTING PHASES

The chirality of superconductivity reflects the internal angular momenta of a Cooper pair. Also other superconducting phases besides the chiral p-wave phase can be found with this property. In this section, we compare the Josephson effect of the p_x+ip_y-wave phase with those of other chiral phase of d- and f-wave origin.

A chiral phase in the case of spin-singlet d-wave symmetry can be composed of the $d_{x^2-y^2}$ and the d_{xy} state, when they are degenerate, yielding a $d_{x^2-y^2}\pm id_{xy}$. This gap function was discussed as the surface states of high-T_c cuparates[35] where the degeneracy is not given, but one of the components is subdominant. The other example is $Na_xCoO_2\cdot yH_2O$.[36] Thus we consider the gap function

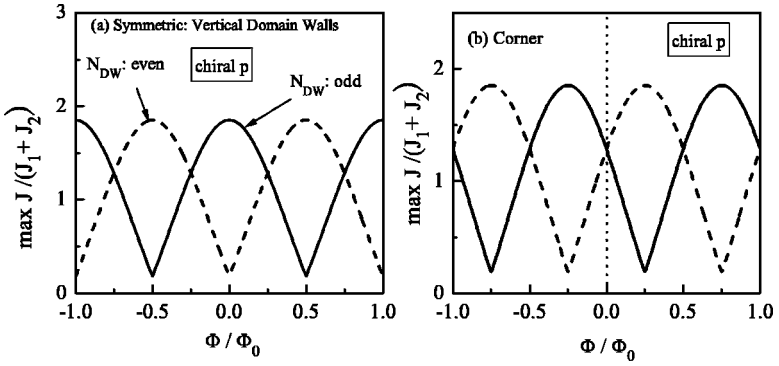

FIG. 6. The critical current in the presence of domain walls for $J_1/J_2=10$. In the symmetric SQUID, the results for the chiral p wave symmetry in the presence of the vertical domain walls are shown in (a). In (b), the critical current for the chiral p wave symmetry in the corner SQUID is shown. The solid (broken) line denote the results when the chirality of the last domain at the bottom is $p_x+ip_y(-p_x+ip_y)$ in (b).

$$\hat{\Delta}_{\boldsymbol{k}}^{(d)} = \{\eta_x(\overline{p_x^2} - \overline{p_y^2}) + \eta_y 2\overline{p_x}\overline{p_y}\} i\hat{\sigma}_2 \tag{23}$$

$$= \Delta(\overline{p_x^2} - \overline{p_y^2} \pm i2\overline{p_x}\overline{p_y}) i\hat{\sigma}_2 = \Delta e^{\pm i2\theta} i\hat{\sigma}_2. \tag{24}$$

Here the coupling to the s-wave superconductor is simpler, since it is not relying on spin-orbit coupling. Thus the current phase relation is dominated by the first-order coupling,

$$J(\phi) = J_d \sin(\phi + 2\theta_n), \tag{25}$$

$$J_d = T_B\left(\frac{\Delta}{2T}\right)\left(\frac{\Delta}{\Delta_0}\right). \tag{26}$$

Concerning the domain wall structure of this state, the two order parameter components behave in the same way as in the p-wave case. Thus only the component perpendicular to the domain wall normal vector changes sign. Thus, for $\boldsymbol{n}\|x$ the component $\eta_y(d_{xy})$ changes sign while $d_{x^2-y^2}$ keeps the phase. Thus, irrespective of the domain wall number for the vertical domain wall case, the maximum of the critical current in the symmetric SQUID would be at $\Phi=0$. Thus, domain walls could not lead to an interference pattern like in the p-wave case. In the case of horizontal domain walls, the situation is more complicated. There is a staggered phase for the $d_{x^2-y^2}$ component. This would give rise to compensating contributions of the two domains to the Josephson effect, similar to the situation discussed in the context of c-axis junction between an s-wave and a twinned high-temperature superconductor.[37,38] In addition, this configuration could give rise to spontaneous half-quanta flux lines wherever a domain wall hits the junction perpendicularly. Under these circumstances, the interpretation of interference pattern would require much more care. Note that such spontaneous fluxes do not occur in the p-wave case as long as the domain wall ends perpendicularly on the junction. In both cases, the flux magnitude depends on the angle between junction interface and domain wall. A similar problem with the domain walls occurs for the corner junction as a simple examination reveals.

The spin-triplet chiral f-wave symmetry is also a possible candidate for the superconducting phase in $Na_xCoO_2 \cdot yH_2O$. The proposed gap function is given by

$$\hat{\Delta}_{\boldsymbol{k}}^{(f)} = i\Delta\{(\overline{p_x^2} - 3\overline{p_y^2})\overline{p_x} \pm i(\overline{p_y^2} - 3\overline{p_x^2})\overline{p_y}\}\hat{\boldsymbol{z}} \cdot \hat{\boldsymbol{\sigma}}\hat{\sigma}_2$$
$$= \Delta e^{\mp i3\theta} i\hat{\boldsymbol{z}} \cdot \hat{\boldsymbol{\sigma}}\hat{\sigma}_2. \tag{27}$$

The current phase relation for the chiral f wave symmetry is given by Eq. (5). In both the symmetric and the corner SQUID, the characteristic behavior of the critical current for the chiral p wave symmetry discussed in Secs. II and III are also valid for the chiral f wave symmetry. In the limit of $J_1/J_2 \gg 1$, the critical current in the symmetric SQUID take the minima at $\Phi=0$ and that in the corner SQUID shows the phase shift by $\pi/4$ in the absence of the domain walls. In addition, there are no differences in effects of domain walls on the critical current between the chiral p wave and the chiral f one. To distinguish the chiral p wave symmetry from the chiral f wave, we should design SQUID's with $\alpha=\pi/3$ or $2\pi/3$.[39] The critical current for f waves becomes symmetric function of Φ and takes its minimum (maximum) at $\Phi=0$ in the SQUID with $\alpha=\pi/3(\alpha=2\pi/3)$,[39] as shown in Fig. 7. On the other hand, the critical current for $J_1/J_2 \gg 1$ in the chiral p wave results in

$$\max|J_{\alpha=\pi/3}(\Phi)| \simeq 2J_1\left|\cos\left(\pi\frac{\Phi}{\Phi_0} - \frac{\pi}{6}\right)\right|, \tag{28}$$

$$\max|J_{\alpha=2\pi/3}(\Phi)| \simeq 2J_1\left|\cos\left(\pi\frac{\Phi}{\Phi_0} - \frac{\pi}{3}\right)\right|. \tag{29}$$

The calculated results are shown in Fig. 7. The asymmetry in the critical current persists in the chiral p wave in such SQUID's. This argument, however, is valid when the differ-

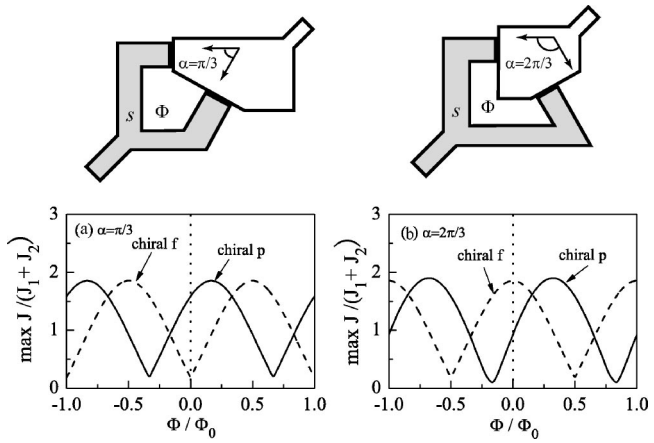

FIG. 7. The critical current for the chiral p wave is compared with that for the chiral f wave in (a) and (b), where $J_1/J_2=10$. The relative junction angle is set at $\alpha=\pi/3$ in (a) and $\alpha=2\pi/3$ in (b) as shown in the upper figures.

ence in the transmission probabilities of the two tunnel junctions in Fig. 7 are much smaller than themselves.

V. DISCUSSION

We have shown that the asymmetry of the critical current with respect to Φ in the corner SQUID is the evidence of the p_x+ip_y symmetry when the period of oscillations is Φ_0. A recent experiment shows a large asymmetry of the critical current in the corner SQUID.[24] The experiment also shows a minima of the critical current around $\Phi=0$ in the symmetric SQUID. The position of minima, however, slightly deviates from $\Phi=0$. We have assumed that J_1 in the left junction is equal to that in the right junction. When those are different from each other, the Josephson critical current becomes asymmetric of Φ even in the symmetric SQUID. Thus the small asymmetry found in the experiment might be caused by the asymmetry of the two tunnel junctions. The degree of asymmetry is negligible when the difference of J_1 in the two junctions is much smaller than themselves.

In addition to p_x+ip_y, the $\sin(p_x)+i\sin(p_y)$[40,41] and $\sin(p_x+p_y)+i\sin(p_x-p_y)$ symmetries[42] have been proposed so far. The perturbation expansion[43,44] also indicates a possibility of the chiral p wave symmetry with more complicated structure than $\sin(p_x)+i\sin(p_y)$ and $\sin(p_x+p_y)+i\sin(p_x-p_y)$. The characteristic behavior of the Josephson current in the two types of SQUID discussed in Secs. II and III are valid not only for the isotropic p_x+ip_y symmetry but also for anisotropic $\sin(p_x)+i\sin(p_y)$ and $\sin(p_x+p_y)+i\sin(p_x-p_y)$ symmetries. The latter two gap function have the fourfold symmetry in the momentum space consistently with a thermal conductivity experiment.[45] In particular, $\sin(p_x+p_y)+i\sin(p_x-p_y)$ is close to the chiral f wave symmetry because $\sin(p_x+p_y)$ and $\sin(p_x-p_y)$ change their sign six times on the Fermi surface. To distinguish one symmetry from another, much more detail analysis would be required. At present, we propose the angle resolved tunneling spectra for this analysis.[46]

VI. CONCLUSION

We have studied the critical Josephson current in two types of SQUID consisting of s wave superconductor and Sr_2RuO_4. In the p_x+ip_y symmetry, the critical Josephson current in the corner SQUID becomes the asymmetric function of Φ because the current-phase relation in the two junctions relate to each other by $\pi/2$ phase shift in the gap function. We also show that the asymmetry remains even in the presence of the chiral domain structures in Sr_2RuO_4. Our results well explain the recent experimental findings.[24]

ACKNOWLEDGMENTS

The authors thank Y. Maeno, Y. Liu, and V. B. Geshkenbein for useful discussion. This work has been partially supported by Grant-in-Aid for the 21st Century COE program on "Topological Science and Technology" from the Ministry of Education, Culture, Sport, Science and Technology of Japan.

*Electronic address: asano@eng.hokudai.ac.jp

[1] J. G. Bednorz and K. A. Müller, Z. Phys. B: Condens. Matter **64**, 189 (1986).
[2] D. A. Wollman, D. J. Van Harlingen, W. C. Lee, D. M. Ginsberg, and A. J. Leggett, Phys. Rev. Lett. **71**, 2134 (1993).
[3] M. Sigrist and T. M. Rice, J. Phys. Soc. Jpn. **61**, 4283 (1992); Rev. Mod. Phys. **67**, 503 (1995).
[4] D. A. Brawner and H. R. Ott, Phys. Rev. B **50**, 6530 (1994).
[5] A. Mathai, Y. Gim, R. C. Black, A. Amar, and F. C. Wellstood, Phys. Rev. Lett. **74**, 4523 (1995).
[6] C. C. Tsuei, J. R. Kirtley, C. C. Chi, Lock See Yu-Jahnes, A. Gupta, T. Shaw, J. Z. Sun, and M. B. Ketchen, Phys. Rev. Lett. **73**, 593 (1994); C. C. Tsuei and J. R. Kirtley, Rev. Mod. Phys. **72**, 969 (2000).
[7] C. R. Hu, Phys. Rev. Lett. **72**, 1526 (1994).
[8] Y. Tanaka and S. Kashiwaya, Phys. Rev. Lett. **74**, 3451 (1995).
[9] J. Geerk, X. X. Xi, and G. Linker, Z. Phys. B: Condens. Matter **73**, 329 (1988).
[10] Y. Asano, Y. Tanaka, and S. Kashiwaya, Phys. Rev. B **69**, 134501 (2004).
[11] S. Kashiwaya and Y. Tanaka, Rep. Prog. Phys. **63**, 1641 (2000).
[12] Y. Maeno, H. Hashimoto, K. Yoshida, S. Nishizaki, T. Fujita, J. G. Bednorz, and F. Lichtenberg, Nature (London) **372**, 532 (1994).
[13] K. Ishida, H. Mukada, Y. Kitaoka, K. Asayama, Z. Q. Mao, Y. Mori, and Y. Maeno, Nature (London) **396**, 658 (1998).
[14] J. A. Duffy, S. M. Hayden, Y. Maeno, Z. Q. Mao, J. Kulda, and G. J. McIntyre, Phys. Rev. Lett. **85**, 5412 (2000).
[15] G. M. Luke, Y. Fudamoto, K. M. Kojima, M. I. Larkin, B. Nachumi, Y. J. Uemura, Y. Maeno, Z. Q. Mao, Y. Mori, H. Nakamura, and M. Sigrist, Nature (London) **394**, 558 (1998).
[16] T. M. Rice and M. Sigrist, J. Phys.: Condens. Matter **7**, L643 (1995).
[17] A. P. Mackenzie and Y. Maeno, Rev. Mod. Phys. **75**, 657 (2003).
[18] F. Laube, G. Goll, H. v. Löhneysen, M. Fogelström, and F. Lichtenberg, Phys. Rev. Lett. **84**, 1595 (2000).
[19] Z. Q. Mao, K. D. Nelson, R. Jin, Y. Liu, and Y. Maeno, Phys. Rev. Lett. **87**, 037003 (2001).
[20] R. Jin, Y. Liu, Z. Mao, and Y. Maeno, Europhys. Lett. **51**, 341 (2000).
[21] C. Honerkamp and M. Sigrist, Prog. Theor. Phys. **100**, 53 (1998).
[22] M. Yamashiro, Y. Tanaka, and S. Kashiwaya, J. Phys. Soc. Jpn. **67**, 3364 (1998).
[23] M. Yamashiro, Y. Tanaka, N. Yoshida, and S. Kashiwaya, J. Phys. Soc. Jpn. **68**, 2019 (1999).
[24] K. D. Nelson, Z. Q. Mao, Y. Maeno, and Y. Liu, Science **306**, 1151 (2004).
[25] V. B. Geshkenbein, A. I. Larkin, and A. Barone, Phys. Rev. B **36**, 235 (1987).
[26] V. B. Geshkenbein and A. I. Larkin, JETP Lett. **43**, 306 (1986)

[JETP Lett. **43**, 395 (1986)].
[27] A. Millis, D. Rainer, and J. A. Sauls, Phys. Rev. B **38**, 4504 (1988).
[28] M. Sigrist and K. Ueda, Rev. Mod. Phys. **63**, 239 (1991).
[29] Y. Asano, Phys. Rev. B **64**, 224515 (2001).
[30] Y. Asano, Y. Tanaka, M. Sigrist, and S. Kashiwaya, Phys. Rev. B **67**, 184505 (2003).
[31] We do not consider spatial dependence of the pair amplitude. Although the amplitude at the interface deviates from its bulk value, effects of spatial dependence in the pair amplitude are negligible in low energy transport such as the Josephson current. See Y. S. Barash, A. M. Bobkov, and M. Fogelström, Phys. Rev. B **64**, 214503 (2001).
[32] A. Barone and G. Paterno, *Physics and Applications of the Josephson Effect* (Wiley, New York, 1982).
[33] Here we assume temperatures are still higher than $\Delta_0 T_B$. When $T \ll \Delta_0 T_B$, the zero-energy state causes the anomalous Josephson effect in the p_x symmetry (see Ref. 30).
[34] M. Sigrist and F. Agterberg, Prog. Theor. Phys. **102**, 965 (1999).
[35] R. B. Laughlin, Phys. Rev. Lett. **80**, 5188 (1998).
[36] M. Ogata, J. Phys. Soc. Jpn. **72**, 1839 (2003).
[37] M. Sigrist, K. Kuboki, P. A. Lee, A. J. Millis, and T. M. Rice, Phys. Rev. B **53**, 2835 (1996).
[38] D. F. Agterberg and M. Sigrist, Phys. Rev. Lett. **80**, 2689 (1998).
[39] J. A. Sauls, Adv. Phys. **43**, 113 (1994).
[40] T. Kuwabara and M. Ogata, Phys. Rev. Lett. **85**, 4586 (2000).
[41] K. Miyake and O. Narikiyo, Phys. Rev. Lett. **83**, 1423 (1999).
[42] R. Arita, S. Onari, K. Kuroki, and H. Aoki, Phys. Rev. Lett. **92**, 247006 (2004).
[43] T. Nomura and K. Yamada, J. Phys. Soc. Jpn. **69**, 3678 (2000).
[44] Y. Yanase and M. Ogata, J. Phys. Soc. Jpn. **72**, 673 (2003).
[45] K. Izawa, H. Takahashi, H. Yamaguchi, Y. Matsuda, M. Suzuki, T. Sasaki, T. Fukase, Y. Yoshia, R. Settai, and Y. Onuki, Phys. Rev. Lett. **86**, 2653 (2001).
[46] D. Tamura, Y. Asano, and Y. Tanaka (unpublished).